DOI: 10.53660/CLM-4316-24V10

A mathematical model describing the tip-stalk regulation in angiogenesis

Um modelo matemático que descreve a regulação tip-stalk na angiogênese

Received: 20-09-2024 | Accepted: 21-10-2024 | Published: 24-10-2024

Dandara Lorrayne do Nascimento
ORCID: https://orcid.org/0000-0003-1169-1575
Center for Technological Education of Minas Gerais (CEFET-MG). Graduate Program in Mathematical and Computational Modeling, Brazil
E-mail: dandara.nascimento@ifsudestemg.edu.br
Ana Paula Alves
ORCID: https://orcid.org/0000-0003-0594-8215
Federal University of Minas Gerais (UFMG). Graduate Program in Physics. State University of Minas Gerais (UEMG), Brazil
E-mail: anafisic@gmail.com
Leonardo Ferreira Calazans
ORCID: https://orcid.org/0000-0003-3320-3587
Center for Technological Education of Minas Gerais (CEFET-MG). Graduate Program in Mathematical and Computational Modeling, Brazil
E-mail: leonardo.ferreira.calazans@gmail.com
Ubirajara Agero
ORCID: https://orcid.org/0000-0002-4987-9031
Federal University of Minas Gerais (UFMG). Graduate Program in Physics, Brazil
E-mail: bira@ufmg.br
Allbens P. F. Atman
ORCID: https://orcid.org/0000-0002-7614-2721
Center for Technological Education of Minas Gerais (CEFET-MG). Graduate Program in Mathematical and Computational Modeling. National Institute of Science and Technology - Complex Systems – INCT, Brazil
E-mail: atman@cefetmg.br

ABSTRACT

Angiogenesis is the process of new blood vessel growth from existing vessels, involving extensive cell signaling. Under normal conditions, new vessels are robust and organized, with a balance among angiogenesis factors. In abnormal conditions, such as tumor development, vessels are stunted and tangled due to an imbalance of these factors. Pathological angiogenesis stimulates rapid vessel growth to feed the oxygen and nutriente starved tumor. Inhibiting angiogenesis can cause side effects like hypertension, thrombosis, and fatigue. To better understand this process, significant effort has gone into studying signaling pathways, contributing to drug development for diseases like cancer. This study presents a mathematical model describing angiogenesis on a microscopic scale, comparing its results with experimental data on vascular network topology. The model, implemented in MatLab®, uses ordinary differential equations to represent cell behavior. Results show that altering VEGF (Vascular Endothelial Growth Factor) disrupts system balance, impacting angiogenesis and possibly explaining differences in network topology seen experimentally.

Keywords: Angiogenesis; Physiological Angiogenesis; Pathological Angiogenesis; Protein Dynamics; Mathematical Modeling.

INTRODUCTION

Angiogenesis is the process that involves the growth, migration, and differentiation of endothelial cells (ECs) (Folkman, 1984; Fouladzadeh et al., 2021). This mechanism is important for wound healing, embryo formation, to direct oxygen and nutrients to cells, among other processes, and is associated with several growth factors (Bhadada, Goyal & Patel, 2011; Nunes et al., 2015).

During angiogenesis, endothelial cells, which are the cells that cover the inner part of blood vessels, lead the growth of new branches (Boareto, Jolly, Ben-Jacob & Onuchic, 2015a). These cells are guided through the extracellular matrix (substance between cells) by chemicals factors that are released in response to nutrient deficiencies in tissues (Boareto et al., 2015a; Kargozar, Baino, Hamzehlou, Hamblin & Mozafari, 2020).

The vascular network formation involves the interaction of cell-cell and cell-matrix extracellular, understanding the chemical mechanism that drives the process and displays different topologies in the vascular network plays an important role to investigate the angiogenesis process.

However, angiogenesis is also related to the emergence of several diseases, as well as the emergence of tumors (Ozel, 2022). Thus, tumor angiogenesis is essential for the development of cancer, acting during growth, progression and metastasis (Qi, Deng, Lian & Yu, 2022).

Studies on the action of angiogenesis in the development of cancer began in the year 1800. On this occasion, German researchers observed that some tumors were richly vascularized, suggesting that the formation of new blood vessels occurred in some cancers (Geindreau, Bruchard & Vegran, 2022).

In this sense, it was discovered that tumor cells also promote angiogenesis by emitting biological signals that indicate hypoxia (Qing, 2022). Therefore, research that seeks to identify pro-angiogenic factors and methods of restricting signaling is of great relevance.

Under normal conditions, new blood vessels are formed in a robust and organized way. And in abnormal conditions, such as when a tumor appears, the vessels formed are excessive, rickety, and tangled. These abnormal conditions lead to the creation of a network of vessels with tight and compromised junctions, as they are stimulated to grow rapidly to feed the tumor that lacks oxygen and nutrients (De Palma & Biziato, 2017; Apte, Chen & Ferrara, 2019). To understand this change, it is necessary to carefully

analyze the conditions that contribute to the accelerated growth of these vessels, in this sense, it is important to study the stimulating factors of angiogenesis.

To investigate the dynamics that drive the angiogenesis process on a microscopic scale, a mathematical model of angiogenesis regulation will be presented, based on the models of Boareto and collaborators (Boareto et al. 2015a; Boareto et al., 2015b). This model will be compared to the experimental study carried out by Alves (Alves, Mesquita, Gómez-Gardenes & Agero, 2018), which proposes to understand the changes promoted in the topology of the vascular network through the restriction of VEGF during the process of vasculogenesis. Therefore, the concentrations of proteins involved in this process will be analyzed to evaluate the possible influence of angiogenic growth factors.

The two signaling pathways acting in angiogenesis will be addressed, which are the cellular and extracellular communication processes: the Notch signaling pathway and the VEGF (Vascular Endothelial Growth Factor) signaling pathway. The Notch signaling pathway, named after the Notch receptor protein, is involved in choosing which cells will lead the new branch of the blood vessel and which cells will form the walls of the new vessel. The VEGF signaling pathway, which takes its name from the signaling factor released by cells that lack oxygen and nutrients, emits pro-angiogenic factors for the growth of these new blood vessels.

The restriction of pro-angiogenic factors has been the subject of studies over the years (Siveen, 2017). However, studies show that attempts to inhibit angiogenesis can cause several side effects in patients, such as high blood pressure, heart failure, arterial thrombotic events, nausea, anxiety, intense pain and sleep disorders (Reiche, Bacal & Mano, 2009; Moreira & Ramos, 2021).

Therefore, research that focuses on describing the angiogenesis process helps investigations aimed at the use of new medicines for various diseases, including cancer. Therefore, this study is necessary, as it will provide quantitative and qualitative data to describe the cellular dynamics involved in angiogenesis. Furthermore, these data may contribute in the future to research that investigates new therapies that minimize the risks and side effects in the treatment of cancer and other diseases.

Several studies, such as those by Leite (2009), Domingues (2010), Silva (2012), Boareto and others (Boareto et al., 2015a; Boareto et al., 2015b), describe the action of tumor angiogenesis through mathematical and computational modeling. This approach makes it possible to effectively understand and characterize biological systems.

According to Freire (2007), computational mathematical models that consider the specific biological variables of the system adequately simulate biological processes faithfully.

Thus, mathematical and computational modeling proves to be effective for investigating the equilibrium state of a dynamic system that describes angiogenesis. Furthermore, the dynamics of the action of the system's proteins can be assessed through modeling. These dynamics, described through first order differential equations, enables understanding when manipulating protein concentrations in the simulation of virtual cells and tissues. This process provides analyses, conjectures, inferences and conclusions about biological functioning.

Therefore, a mathematical model for angiogenesis will be presented, based on first order differential equations, which describes the dynamics of proteins considering a single cell in the middle of an external environment in which the different concentrations present are simulated.

NOTCH AND VEGF SIGNALING PATHWAYS

One of the receptor proteins that act in the angiogenesis process is Notch. Notch is a transmembrane protein (which covers the cell membrane from one side to the other) that plays an important role in cell fate (Ross & Kadesch, 2001). Its signaling pathway is one of the most investigated due to its versatility in the cellular communication process (Jarriault, et al., 1995; Liao & Oates, 2017; Andersson, Sandberg & Lendahl, 2011).

The Notch signaling pathway has a direct route between the membrane and the cell nucleus and presents cell-cell communication. In this process, transmembrane binding proteins from an external environment activate the cell's receptor proteins (Siebel & Lendahl, 2017).

Around 110 years ago, studies on Notch began and today it is known that Notch signaling participates in several biological processes between species, such as organ formation and tissue function. Therefore, the malfunction of this signaling may indicate a pathological environment (Zhou et al., 2022).

Some studies show that the Notch signaling pathway is much more extensive and complex than previously believed (Sarin & Marcel, 2017; Polacheck et al., 2017). As immunotherapy has revolutionized cancer treatment, the Notch signaling pathway and its relationship with angiogenesis has attracted the attention of scientists (Zhou et al., 2022).

In this sense, there is also the binding protein Delta that acts in the angiogenesis process. Delta has been identified as a potentially important target in tumor angiogenesis (Patel et al., 2005). Studies on tumors in mice and humans have shown that Delta is strongly expressed in tumor angiogenesis compared to physiological angiogenesis (Thurston & Kitajewski, 2008).

Thus, the binding between Notch and Delta allows the NICD to migrate to the nucleus of the cell containing Notch of the binding and restrict the rate of production of new Delta proteins but increase the rate of protein production Notch (Thurston & Kitajewski, 2008).

Notch-Delta signaling causes neighboring cells to acquire opposite patterns. That is, a cell with high Delta and low Notch promotes that its neighboring cells have high Notch and low Delta on its surface. This pattern is called lateral inhibition and ensures that cells differentiate into distinct fates from an initially homogeneous cell population (Beatus & Lendahl, 1998; Troost, Binshtok, Sprinzak & Klein, 2023). Cells with high Delta are called emitters and cells with high Notch are called receivers (Boareto et al., 2015b).

In addition to the Delta ligand, there is the Jagged ligand protein that also acts in the angiogenesis process. Research reveals that the excessive increase in Jagged is related to tumor angiogenesis, as well as some types of cancer such as breast and ovarian (Funahashi et al., 2008; Zhou et al., 2022). The study carried out in 1997 and presented in Li et al. (1997) shows that the Jagged mutation is also related to the development of Alagille Syndrome, which is an autosomal dominant disease characterized by abnormal development of organs.

In this sense, the connection between Notch and Jagged allows the NICD to migrate to the nucleus of the cell that contains Notch of the connection and increase the production rates of Notch and Jagged simultaneously (Boareto et al., 2015a; Bocci, Onuchic & Jolly, 2020). Notch-Jagged signaling promotes neighboring cells to acquire similar patterns. That is, cells with high Jagged and high Notch, being called Sender/ Receiver hybrid phenotypes, to highlight that both cells send and receive signals (Boareto et al. 2015b). This pattern is called lateral induction and guarantees similar cell fates (Bocci et al., 2020).

If the connection between Notch and Delta, or between Notch and Jagged, with between different cells, there is a trans activation. However, if it occurs in the same cell,

there is cis inhibition and, in this case, the NICD is not activated and both proteins are degraded in the process (Boareto et al., 2015a; Boareto et al., 2015b).

In addition to the characteristics presented here, Boareto et al. (2015a) consider another factor called the fringe effect, which divides the Notch population into two parts, making one of them more susceptible to receiving Delta instead of Jagged.

In the Notch signaling pathway, fringe acts to coordinate binary cell fate decisions during angiogenesis (LoPilato et al., 2023). Furthermore, growing evidence has highlighted fringe's role in cancer, suggesting that its modulation may reduce cancer cell proliferation (Cheng, Oon, Kaur, Sainson & Li, 2022).

In this sense, cells with a high concentration of Jagged emit signals that suppress the activation of Notch modified by fringe, so that the expression Notch-Delta is reinforced (LoPilato et al., 2023). In this scenario, loss of regulation of the pathway by Notch-Jagged signal suppressed by fringe causes destabilization of cell fate tip (LoPilato et al., 2023).

Another very important signaling pathway in the angiogenesis process is VEGF (Vascular Endothelial Growth Factor). Tumor angiogenesis has become important for researchers aiming to develop antitumor therapies, with most therapies aimed at blocking the VEGF signaling pathway (Thurston & Kitajewski, 2008).

VEGF family proteins are regulators of angiogenesis, both in physiological circumstances and in a pathological condition (Thurston & Kitajewski, 2008). Thus, there is the VEGF- A binding protein, also named simply as VEGF, and the VEGFR-2 receptor protein, also named as VEGFR2 or VEGF-2 (Shibuya, 2011).

In VEGF signaling, the VEGF-A ligand, found on the outside of the cell, activates the VEGFR2 receptor, stimulating angiogenesis. Although VEGF is essential to maintain the relative condition of stability in cells and tissues, the importance of this factor for tumor growth and metastasis dissemination has been demonstrated (Apte et al., 2019). Furthermore, Boareto et al. (2015a) and Boareto et al. (2015b) showed a great influence of the Jagged protein in the Notch signaling for the appearance of tumors.

In the process of new blood vessel growth, the endothelial cell that leads the growth of the new vessel is called a tip cell, and new thin extensions (phyllopods) are created in this cell to follow the signalings emitted by VEGF-A. The remaining cells that follow the tip cell proliferate and form the stem of the new blood vessel. Those are the stalk cells. As has been shown the mechanical regulation of cells in angiogenesis process gives rise to the mean of chemical transduction (Flournoy, Ashkanani & Chen, 2022).

Tissues rich in proteins Delta and VEGFR2 give rise to tip cells and, tissues rich in proteins Jagged, NICD and Notch, give rise to cells stalk. The vessels emerge using a well regulated balance between the migration of tip cells and the proliferation of stalk cells (Geudens & Gerhardt, 2011). As has been shown the Jagged plays an important role in tumor progression (Boareto et al., 2016). To understand the vascular network formation many mathematical models have been proposed to study the cell's interactions (Scianna, Bell & Preziosi, 2013). On the other hand, there are many factors involved in the microscopic scale that drives the behavior in the macroscopic scale that still not understand. So, this work proposes a model that describes how the possible single cell interactions give rise to the macroscopic behavior in the angiogenesis process.

The high concentration of Delta and VEGFR2 in the tip cell causes its neighbors to acquire an opposite pattern (with low Delta and VEGFR2) called lateral inhibition. On the other hand, the high concentration of Jagged, NICD, and Notch in the stalk cell causes its neighbors to acquire a similar pattern, called lateral induction, which will promote vessel elongation. The interaction between the VEGF and Notch signaling pathways is important to define the fate of tip and stalk cells.

Studies show that composite cells with tip/stalk characteristics promote the emergence of tumor angiogenesis, as there is competition between the position of guiding new vessels towards VEGF-A (Boareto et al., 2015a; Nascimento, 2021). This causes blood vessels to grow faster, poorly perfused and disorganized.

VASCULAR NETWORK TOPOLOGY

The study presented by Alves et al. (2018) analyzes the formation of the vascular network in chicken embryos of the species gallus gallus domesticus. The embryos were divided equally into two distinct groups: the control group (used to extract quantitative parameters) and the group treated with 30µL of Avastin® (Bevacizumab or Bevacizumabe) at a concentration of 6µg/µL (used to verify the influence of VEGF on vascular network development).

Avastin® is an antibody used in chemotherapy treatments and inhibits the action of VEGF. According to Mukerjee (2010), Avastin® is applied to inhibit angiogenesis, and its use in early stage tumors has been studied over the years. Before that, Avastin® was widely used to treat metastases.

When Avastin® is added to the system, it receives the VEGF-A ligand contributing so that the signaling between VEGFR2 and VEGF-A is not activated and, consequently, angiogenesis is slowed down. When there is no influence of the drug on the system, the link between VEGFR2 and VEGF-A forms the VEGFR + VEGF-A set, which enables the activation of angiogenesis (Alves et al., 2018).

The main result presented in Alves et al. (2018) is that the network topologies obtained for the two groups of embryos showed differences, as shown in Figure 1.

Figure 1 – Network topology

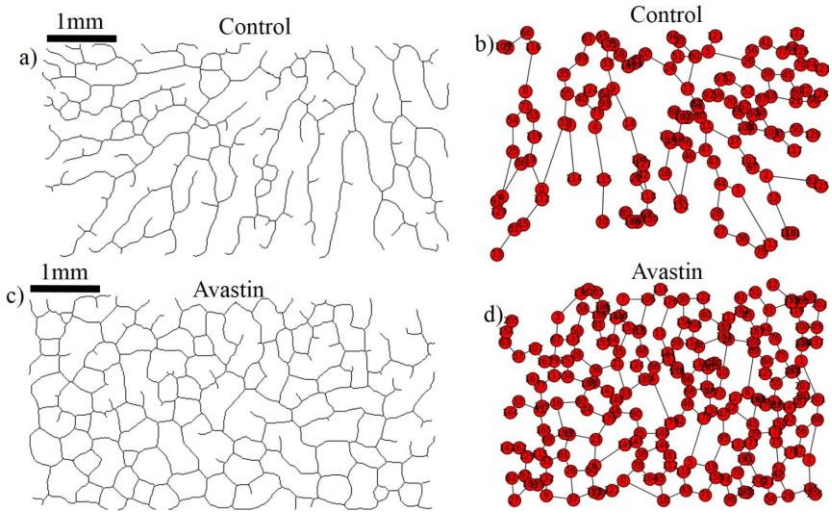

Source: Alves et al. (2018)

In the control group, VEGF binds to molecules presents in the extracellular matrix and enables the formation of pathways that stimulate the migration of endothelial cells, forming a tree like vascularization (Figure 1a-b). In samples treated with Avastin®, it is observed that a symmetry break of the bonds occurs (Figure 1 c-d)(Alves et al., 2018). This is an indication that VEGF-A, present in the extracellular matrix, binds to Avastin® and the bindings in this type of sample do not follow the same paths as in the control group. On a treated group probably happen a random vascular network connections and the topology observed at final stage displays a lattice like vascular topology. This statement corroborates what was seen in the descriptions presented in Boareto et al. (2015a), as VEGF induces the formation of new shoots, and the cell tip migrates towards the signal emitted by VEGF leading to a new angiogenic branch. Furthermore, studies suggest that tumors treated with antiangiogenic drugs have their vascular network reorganized to improve oxygenation and drug penetration into the system (Jain, 2005).

Through a complete mechanism, several factors influence the promotion or inhibition of angiogenesis (Huang & Nan, 2019). Therefore, theoretical work seeks to understand how the dynamics of blood vessel formation occur. Theoretical studies such as those presented in Boareto et al. (2015a) and Boareto et al. (2015b) investigate the microscopic mechanisms of cellular chemistry involved in the growth of the vessels that feed a tumor. This research can contribute to the search for less invasive drugs that focus on restricting the processes that, in tumors, lead to the unrestrained proliferation of blood vessels (Kargozar, 2020).

MATHEMATICAL MODEL

The signaling pathway Notch is activated when the receiver Notch receives the binders Delta or Jagged. When Notch receives Delta, the NICD is activated and, in the nucleus of the cell containing Notch the production rate of Notch is increased, but the production rate of Delta is restricted. When Notch receives Jagged the NICD is also activated and in the cell nucleus causes both Notch and Jagged to have their production rates increased. When the receptor and ligands interact between different media, or different cells, the NICD is activated, and this dynamic is called trans activation. However, when the receptor and ligands interact in the same cell, the NICD is not activated, the proteins involved in the process are degraded and this dynamic is called cis inhibition (Boareto et al., 2015a; Boareto et al., 2015b) (Figure 2).

Moreover, there is also the VEGFR2 receptor and the VEGF-A ligand. When VEGFR2 receives VEGF-A, the NICD is activated and in the cell nucleus causes the production rate of Delta to be increased and the production rate of VEGFR2 to be restricted (Boareto et al., 2015a; Boareto et al., 2015b) (Figure 2).

Considering this dynamic, it is noteworthy that cells with high concentrations of Delta and VEGFR2 and with low concentrations of NICD and Jagged are called tip cells, which are cells that migrate towards VEGF-A, thus guiding the formation of new blood vessels. However, cells with high concentrations of NICD and Jagged and with low concentrations of Delta and VEGFR2 are called stalk cells, which form the wall of new blood vessels (Boareto et al., 2015a).

Figure 2 – Representation of a cell interacting with the external environment.

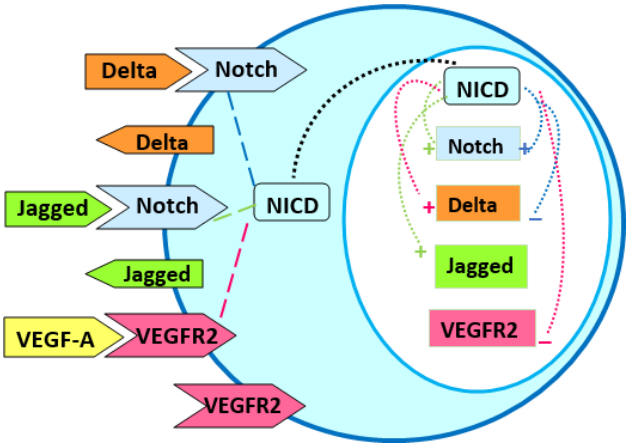

The mathematical model that will be presented is adapted from Boareto et al. (2015a). In the model presented in Boareto et al. (2015a) a phenomenon called the fringe effect is considered. It is an effect that modifies part of the Notch population to make it more apt of receiving Delta instead of Jagged. Contrary to what was done in Boareto et al. (2015a), the fringe effect will not be considered in the mathematical model developed in this research, in order to evaluate its possible qualitative influence on the system, and, for this, the results of the system dynamics will be compared with the results presented in Boareto et al. (2015a).

Therefore, when considering the dynamics described and presented in Figure 2, the mathematical model adapted from Boareto and collaborators Boareto et al. (2015a) is represented by the following equations:

$$\frac{dN}{dt} = N_0 H^{s+}(I, \lambda_{I,N}) - N[(k_c D + k_t D_{ext}) + (k_c J + k_t J_{ext})] - \gamma N \quad (1)$$

$$\frac{dD}{dt} = D_0 H^{s-}(I, \lambda_{I,D}) H^{s+}(V, \lambda_{V,D}) - D[k_c N + k_t N_{ext}] - \gamma D \quad (2)$$

$$\frac{dJ}{dt} = J_0 H^{s+}(I, \lambda_{I,J}) - J[k_c N + k_t N_{ext}] - \gamma J \quad (3)$$

$$\frac{dI}{dt} = k_t N[D_{ext} + J_{ext}] - \gamma_I I \quad (4)$$

$$\frac{dV}{dt} = k_t V_R V_{ext} - \gamma_I V \quad (5)$$

$$\frac{dV_R}{dt} = V_{R0} H^{s-}(I, \lambda_{I,VR}) - k_t V_R V_{ext} - \gamma V_R \quad (6)$$

where $N, D, I, J, V,$ and VR represent, respectively, the concentrations of the proteins Notch, Delta, NICD, Jagged, VEGF and VEGFR2. N_0, D_0, J_0 e VR_0 represent, respectively, the production rates of Notch, Delta, Jagged and VEGFR2 which are enlarged or restricted in the cell nucleus. The term k_t represents the trans interaction and the term k_c represents the cis inhibition. N_{ext} , D_{ext}, J_{ext} and V_{ext} represent, respectively, the external cell concentrations of the proteins Notch, Delta, Jagged and VEGF (which is VEGF-A). Also, γ and γI γ_I are the natural degradation rates of proteins. The term $H^{s+}(I, \lambda_{I,N})$ represents the shifted Hill equation, which causes the production rate of Notch to be increased in the kernel, due to the action of the NICD. In a similar way, $H^{s-}(I, \lambda_{I,D})$ represents the shifted Hill equation that constrains the production of Delta in the kernel under the action of the NICD and $H^{s+}(V, \lambda_{V,D})$ represents the increase of Delta in the cell nucleus via the VEGF signaling pathway. The term $H^{s+}(I, \lambda_{I,J})$represents the shifted Hill equation that regulates the increase of Jagged in the kernel through the action of the NICD. The shifted Hill equation that constrains the production rate of VEGFR2 is given by $H^{s-}(I, \lambda_{I,VR})$. For details on constructing the model equations, see Appendix A.

Therefore, the model is composed of six equations, each of which represents the dynamics of a protein present in the angiogenesis process.

It is noteworthy that the model equations describe the concentrations present in a single cell, which is immersed in an external environment where the other external concentrations are simulated.

MATERIAL AND METHODS

Initially, a detailed study was carried out on the mathematical models, which correspond to angiogenesis, developed by Boareto et al. (2015a) and Boareto et al. (2015b). Contrary to what was done by these authors, in the mathematical model developed in this research, the fringe effect was not considered as a way of verifying whether it influences the results obtained, which will be compared with those presented in literature.

The mathematical model obtained was compared to the experimental study of Alves et al. (2018). From the action performed by VEGF-A in angiogenesis, these results

were associated with the results regarding the formation of the topology of the vascular network presented in Alves et al. (2018).

All mathematical models were built using first order differential equations when considering the dynamics of the Notch and VEGF signaling pathways.

To perform the computational analyses, the data processing was done using MatLab® software.

To analyze the model's equilibrium solutions, the equations were linearized, the Jacobian matrix was calculated and the eigenvalues were found to determine the stability of each equilibrium point.

To validate the model, the analyzes performed were compared with the investigations carried out in Boareto et al. (2015a) and Boareto et al. (2015b) and reproduced the same qualitative behavior, even not considering the fringe effect in the model as proposed here.

RESULTS AND DISCUSSIONS

Equilibrium Analysis:

Using the model equations and the parameters presented in Appendix A.2, Figure 3 presents the dynamics of the system's proteins and the nullclines without the influence of VEGF.

Figure 3a) presents the concentrations of values reached by proteins of the Notch signaling pathway, without the influence of VEGF. It is observed that the production of the binding protein Jagged is the highest in the system. Furthermore, the concentration of Delta binding proteins is greater than that of the Notch receptor and NICD. This reflects a state of high concentration of binding proteins. It should be noted that this dynamic is obtained for a particular set of conditions for N_0, D_0, J_0 and I_0.

Figure 3 – Dynamics and equilibrium points of the model in the absence of VEGF.

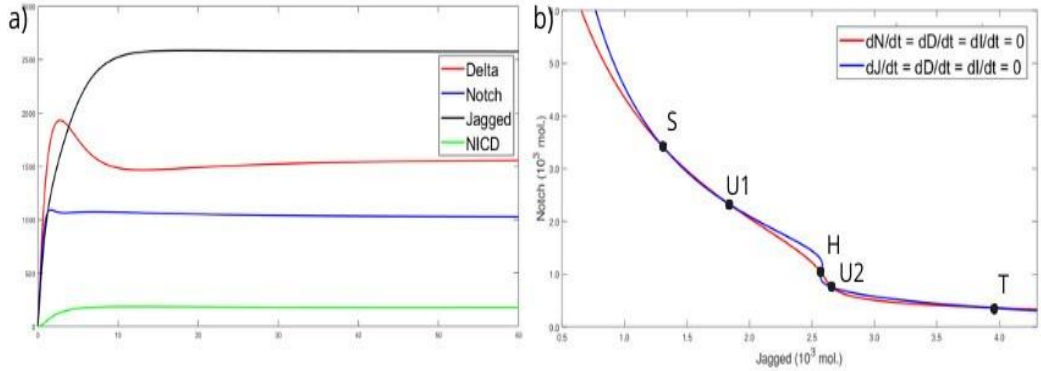

Figure 3a) shows signaling growth behavior in the absence of VEGF. Figure 3b) shows Notch versus Jagged and the existence of five equilibrium points is observed, which are the points where the two curves intersect. These equilibrium points will be called S, U1, H, U2 and T. Below, $\vec{x}_1, \vec{x}_2, \vec{x}_3, \vec{x}_4$ and $\vec{x}_5$ present the concentrations of each protein in S,U1, H, U2 and T, respectively.

$$\vec{x}_1 = \begin{bmatrix} N \\ D \\ J \\ I \end{bmatrix} = \begin{bmatrix} 3385{,}2 \\ 101{,}3 \\ 1317{,}5 \\ 592{,}4 \end{bmatrix}, \vec{x}_2 = \begin{bmatrix} N \\ D \\ J \\ I \end{bmatrix} = \begin{bmatrix} 2329{,}2 \\ 270{,}8 \\ 1835{,}3 \\ 407{,}6 \end{bmatrix}, \vec{x}_3 = \begin{bmatrix} N \\ D \\ J \\ I \end{bmatrix} = \begin{bmatrix} 1025{,}7 \\ 1562{,}9 \\ 2573{,}7 \\ 179{,}5 \end{bmatrix},$$

$$\vec{x}_4 = \begin{bmatrix} N \\ D \\ J \\ I \end{bmatrix} = \begin{bmatrix} 751{,}1 \\ 2511{,}4 \\ 2659{,}2 \\ 131{,}4 \end{bmatrix}, \vec{x}_5 = \begin{bmatrix} N \\ D \\ J \\ I \end{bmatrix} = \begin{bmatrix} 360{,}2 \\ 5367{,}2 \\ 3945{,}6 \\ 63 \end{bmatrix}$$

Now, the stability of points S, U1, H, U2 and T, presented in Figure 3b) will be mathematically evaluated. According to Sayama (2015), after finding the equilibrium points, the next step to analyze the linear stability of continuous time nonlinear systems is to calculate the Jacobian matrix. When using the parameters presented in Appendix A.2 and calculating the partial derivatives to compose the Jacobian matrix J, we have:

$$J = \begin{bmatrix} -\frac{\mathrm{D}}{2*10^3} & -\frac{J}{2*10^3} & -\frac{3}{16} & -\frac{N}{2*10^3} & -\frac{N}{2*10^3} & \frac{4\,\mathrm{I}}{25\,\sigma_2} & -\frac{2\,\mathrm{I}}{25\,{\sigma_2}^2} & -\frac{\mathrm{I}^3}{25*10^4\,{\sigma_2}^2} \\ -\frac{\mathrm{D}}{2*10^3} & & \sigma_3 & 0 & & -\frac{9\mathrm{I}}{10^2\,{\sigma_2}^2} & & \\ -\frac{J}{2*10^3} & & 0 & \sigma_3 & \frac{\sigma_4}{8*10^7\,\sigma_1} & -\frac{\sigma_4}{16*10^7\,{\sigma_1}^2} & -\frac{3\mathrm{I}^9}{256*10^{17}\,{\sigma_1}^2} & \\ \frac{7}{80} & & 0 & 0 & & -\frac{1}{2} & & \end{bmatrix}$$

Where $\sigma_1 = \frac{I^5}{32*10^{10}} + 1, \sigma_2 = \frac{I^2}{4*10^4} + 1, \sigma_3 = -\frac{N}{2*10^3} - \frac{1}{8}$ and $\sigma_4 = 3I^4$.

After substituting the equilibrium values, presented by $\vec{x}_1, \vec{x}_2, \vec{x}_3, \vec{x}_4$ and $\vec{x}_5$, in the Jacobian matrix, they were found the following eigenvalues:

$$\vec{x}_1(\Lambda) = \begin{bmatrix} -2{,}5365 \\ -0{,}0367 \\ -0{,}6413 \\ -1{,}8176 \end{bmatrix}, \vec{x}_2(\Lambda) = \begin{bmatrix} -2{,}3767 \\ 0{,}0321 \\ -0{,}6855 \\ -1{,}2896 \end{bmatrix}, \vec{x}_3(\Lambda) = \begin{bmatrix} -2{,}9067 \\ -0{,}0556 \\ -0{,}4314 \\ -0{,}6379 \end{bmatrix}, \vec{x}_4(\Lambda) = \begin{bmatrix} -3{,}7782 \\ 0{,}0344 \\ -0{,}5296 \\ -0{,}5005 \end{bmatrix}, \vec{x}_5(\Lambda) = \begin{bmatrix} -5{,}0952 \\ -0{,}0596 \\ -0{,}4991 \\ -0{,}3051 \end{bmatrix}$$

The last step refers to the analysis of stability according to the eigenvalues obtained.

In this sense, the dominant eigenvalue of $\vec{x}_1(\Lambda)$ is $\vec{x}_1(\Lambda) < 0$, of $\vec{x}_3(\Lambda)$ is $-0{,}0556 < 0$ and $\vec{x}_5(\Lambda)$ of $-0{,}0596 < 0$. Therefore, these are stable equilibrium points. This means that even when adding a small perturbation in the vicinity of each of

these equilibrium points, the protein concentrations tend to return to the equilibrium values given in $\vec{x}_1(\Lambda), \vec{x}_3(\Lambda)$ and $\vec{x}_5(\Lambda)$.

In $\vec{x}_2(\Lambda)$ the dominant eigenvalue is $0{,}0321 > 0$ and in $\vec{x}_4(\Lambda)$ the dominant eigenvalue is $0{,}0344 > 0$. In this case, the points equilibrium points are unstable and, furthermore, as the other eigenvalues are less than zero, these equilibrium points are saddle points. As equilibria are unstable, this means that when adding a small perturbation in the vicinity of these points, the system tends to move infinitely away from the concentrations presented in $\vec{x}_2(\Lambda)$ and in $\vec{x}_4(\Lambda)$. However, an unstable equilibrium point can come with other eigenvalues that show stability, as is this case. At the saddle point, nearby trajectories are attracted to the equilibrium point in some directions but are repelled in other directions (Sayama, 2015).

When checking the concentrations of proteins present at the stable equilibrium point S, high concentrations of Notch and Jagged proteins were found. Furthermore, low concentrations of Delta. Therefore, point S has characteristics of stalk cells, which are the cells that will compose and lengthen the walls of blood vessels, corroborating the results obtained in (Boareto et al., 2015a).

When analyzing the values achieved for each protein at point T, it was observed that the stable equilibrium point T has a high concentration of protein Delta and a low concentration of Notch. Therefore, it can be concluded that this point characterizes tip cells, which are the cells that will guide the growth of new blood vessels, corroborating the results obtained in (Boareto et al., 2015a).

Finally, when analyzing the concentrations at point H, a new state for the system was discovered. The asymmetry of the NICD in restricting Delta and increasing Jagged production is responsible for the emergence of this hybrid stable equilibrium state, which causes cells to acquire similar fates, being receptors and ligands at the same time (Boareto et al., 2015b). The analyzes showed that for this point there are intermediate concentrations of the Notch repeater and the Delta and Jagged ligands, as found in (Boareto et al., 2015b). Therefore, this stable equilibrium point with hybrid concentrations allows the cell to emit and receive signals, having characteristics of receptor and ligand at the same time (Boareto et al., 2015b). In this hybrid state, cells will have tip and stalk characteristics at the same time, which can lead to a pathological state of angiogenesis, where their states compete for the position of guiding the growth of new blood vessels to supply the body of oxygen.

Introducing the VEGF signaling pathway to the analyses, using the model equations, and the parameters presented in Appendix A.2, Figure 4 presents the dynamics and equilibrium points of the system.

Figure 4 – Dynamics and equilibrium points of the model.

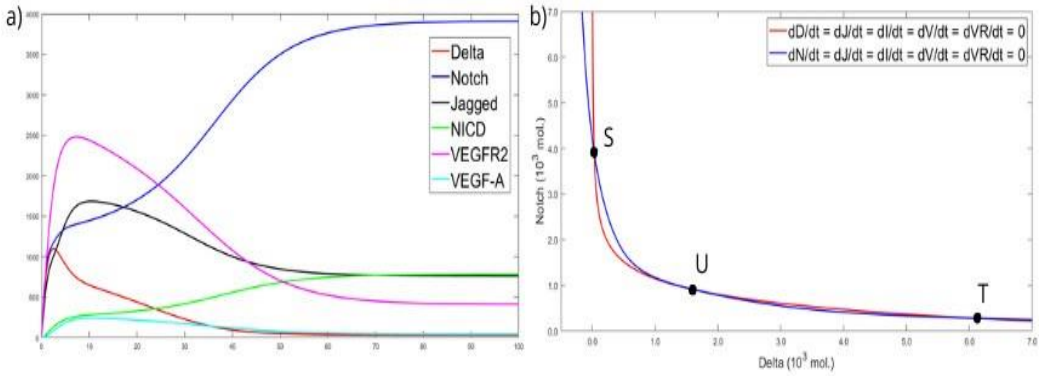

Figure 4a) shows the concentrations of values reached by proteins from the Notch and VEGF signaling pathways. It is observed that the concentration of Notch receptor protein is predominant in the model. Furthermore, the concentrations of Jagged and NICD are predominant in relation to the concentrations of VEGFR2, Delta and VEGF. Given the specific parameters used, this dynamic represents a state of concentration of stalk cells, which are the cells that lengthen the formation of the walls of new blood vessels It can be concluded that the model reproduces the expected behavior, that is, NICD favors the production of Notch and Jagged, however Notch stabilizes with a higher value than Jagged because the production rates of these proteins are different and $N_0 > J_0$. On the other hand, NICD inhibits the production of Delta which could be favored if the VEGF concentration was high; however, VEGF growth is also inhibited by NICD.

It should be noted that this result reflects behavior for a particular set of conditions for N_0, D_0, J_0, I_0 and VR_0 and in it, a high concentration of Notch is noted, which represents a state of cells stalk.

Figure 4b) shows Notch versus Delta and the existence of three equilibrium points is observed, which are the points where the two curves intersect. These equilibrium points will be called S, U and T. Below, $\vec{x}_1, \vec{x}_2$ and $\vec{x}_3$ present the concentrations of each protein in S, U and T, respectively.

$$\vec{x}_1 = \begin{bmatrix} N \\ D \\ J \\ I \\ V \\ VR \end{bmatrix} = \begin{bmatrix} 274{,}2 \\ 6173{,}5 \\ 2790{,}7 \\ 54{,}8 \\ 620 \\ 6200{,}4 \end{bmatrix}, \vec{x}_2 = \begin{bmatrix} N \\ D \\ J \\ I \\ V \\ VR \end{bmatrix} = \begin{bmatrix} 900{,}9 \\ 1628{,}8 \\ 1828{,}5 \\ 180{,}2 \\ 368 \\ 3679{,}8 \end{bmatrix}, \vec{x}_3 = \begin{bmatrix} N \\ D \\ J \\ I \\ V \\ VR \end{bmatrix} = \begin{bmatrix} 3909 \\ 30{,}4 \\ 759{,}9 \\ 781{,}8 \\ 40{,}9 \\ 409{,}5 \end{bmatrix}$$

Now, the stability of points S, U and T, presented in Figure 4b) will be evaluated mathematically. When using the parameters presented in Appendix A.2 and calculating the partial derivatives to compose the Jacobian matrix J, we have:

$$J = \begin{bmatrix} -\frac{D}{2*10^3} & -\frac{J}{2*10^3} & -\frac{1}{5} & -\frac{N}{2*10^3} & -\frac{N}{2*10^3} & \frac{3I}{25\sigma_2} & -\frac{3I}{50{\sigma_2}^2} & -\frac{3I^3}{10^6{\sigma_2}^2} & 0 & 0 \\ -\frac{D}{2*10^3} & \sigma_4 & 0 & & & -\frac{I\left(\frac{1}{\sigma_1}+\frac{V^2}{2*10^4\sigma_1}\right)}{20{\sigma_2}^2} & & & -\frac{10^3\left(\frac{V}{2*10^4{\sigma_1}^2}-\frac{V}{10^4\sigma_1}+\frac{V^3}{4*10^8{\sigma_1}^2}\right)}{\sigma_2} & 0 & 0 \\ -\frac{J}{2*10^3} & 0 & \sigma_4 & \frac{I^4}{4*10^7\sigma_3} & -\frac{I^4}{8*10^7{\sigma_3}^2} & -\frac{I^9}{128*10^{17}{\sigma_3}^2} & & & 0 & 0 \\ \frac{1}{10} & 0 & 0 & & & -\frac{1}{2} & & & 0 & 0 \\ 0 & 0 & 0 & & & 0 & & & -\frac{1}{2} & \frac{1}{20} \\ 0 & 0 & 0 & & & -\frac{I}{20{\sigma_2}^2} & & & 0 & -\frac{3}{20} \end{bmatrix}$$

Where $\sigma_1 = \frac{V^2}{4*10^4} + 1, \sigma_2 = \frac{I^2}{4*10^4} + 1, \sigma_3 = \frac{I^5}{32*10^{10}} + 1$ and $\sigma_4 = -\frac{N}{2*10^3} - \frac{3}{20}$.

After substituting the equilibrium values, presented by $\vec{x}_1, \vec{x}_2$ and $\vec{x}_3$, in the Jacobian matrix, they were found the following eigenvalues:

$$\vec{x}_1(\Lambda) = \begin{bmatrix} -4{,}8780 \\ -0{,}0838 \\ -0{,}1610 \\ -0{,}5243 \\ -0{,}4722 \\ -0{,}2871 \end{bmatrix}, \vec{x}_2(\Lambda) = \begin{bmatrix} -2{,}5054 \\ 0{,}0217 \\ -0{,}5911 \\ -0{,}2325 \\ -0{,}3719 \\ -0{,}6005 \end{bmatrix}, \vec{x}_3(\Lambda) = \begin{bmatrix} -2{,}5035 \\ -0{,}1109 \\ -0{,}1623 \\ -0{,}5808 \\ -0{,}4922 \\ -2{,}1045 \end{bmatrix}$$

In this sense, the dominant eigenvalue of $\vec{x}_1(\Lambda)$ is $-0{,}0838 < 0$ and of $\vec{x}_3(\Lambda)$ is $-0{,}1109 < 0$. Therefore, these are stable equilibrium points. In $\vec{x}_2(\Lambda)$ the dominant eigenvalue is $0{,}0217 > 0$. In this case, the equilibrium is unstable and, furthermore, as the other eigenvalues are less than zero, this is a saddle point.

By analyzing the values achieved for each protein at point T, it was observed that the stable equilibrium point T has a high concentration of Delta binding protein and VEGFR2 receptor protein. In addition, there are low concentrations of Notch receptor protein and Jagged binding protein at the T spot. Therefore, it can be concluded that this spot configures tip cells, which are the cells that will guide the growth of new blood vessels, corroborating the results obtained in (Boareto et al., 2015a).

When verifying the concentrations of proteins present at the stable equilibrium point S, high concentrations of Notch receptor protein, Jagged binding protein, and NICD

were found. In addition, low concentrations of Delta binding protein, VEGFR2 receptor protein, and VEGF were observed. Therefore, point S has characteristics of stalk cells, which are the cells that will compose and lengthen the walls of blood vessels, corroborating the results obtained in (Boareto et al., 2015a).

Using this model and the parameters adopted in Boareto et al. (2015a) it was possible to obtain consistent results even without using the fringe effect. Therefore, the model proposed here is considered functional and simpler than the one suggested by Boareto et al. (2015a).

Finally, the results presented in Figure 4 deserve to be highlighted, as there are fixed points that describe the states that will be seen later in the study by Alves et al. (2018).

The Influence of VEGF-A in the Model:

When cells need oxygen and nutrients, chemical factors such as VEGF-A are released to signal this deficiency. In response to this signaling, the tip cell migrates towards the VEGF-A ligand guiding the formation of the new blood vessel that will carry oxygen and nutrients to these cells (Boareto et al., 2015a; Kargozar et al., 2020).

The study presented by Alves et al. (2018) experimentally shows the role of VEGF- A inhibition in the vascular network growth process. However, it is important to mathematically understand the influence of this factor on the angiogenesis process.

By varying the value of VEGF-A (V_{ext}) in the model and keeping the other parameters, we have the Figure 5.

Figure 5 – Phase representation.

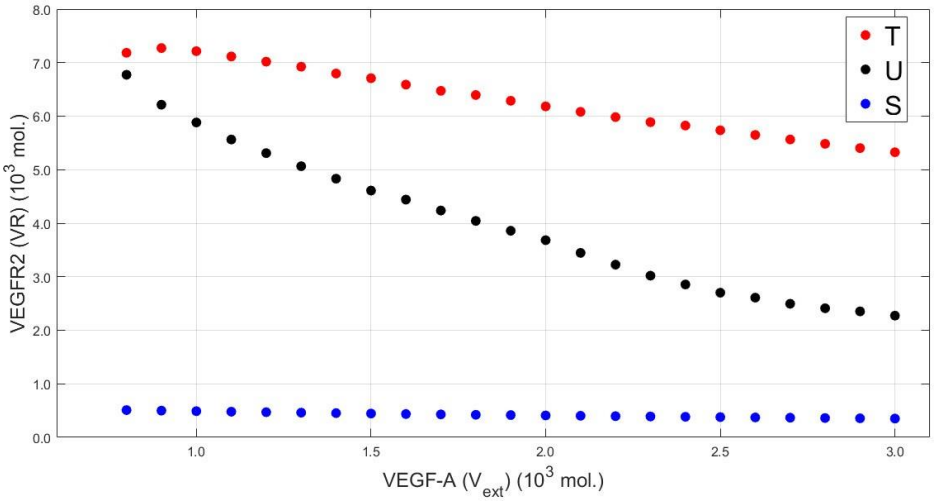

Figure 5 characterizes the plot of VEGFR2 versus VEGF-A, in which the values of VEGF-A were varied from 800 to 3000 molecules, in intervals of 100 molecules. Each point represented in Figure 5 presents new equilibrium concentrations for the model proteins.

For each new VEGF-A value, three new coordinates were obtained for the three equilibrium points. These new points referring to new VEGF-A concentrations maintained the same characteristics observed in Figure 4 (unstable U, stable T and stable S). Therefore, the analysis showed that the points called tip and stalk are stable and represent tip and stalk cells, respectively. Furthermore, the equilibrium point U is unstable, sometimes tending to the stalk point and sometimes tending to the tip point. This shows that the same characteristics were maintained when taking V_{ext} = 2000 molecules. However, the protein concentrations in each system were altered. In Figure 5, it is observed that the higher the value of VEGF-A, the lower the concentration of VEGFR2 in the system. This fact is explained by the junction between VEGF-A and VEGFR2, forming the key that makes the receptor active, decreasing the concentration of free VEGFR2. Furthermore, according to Boareto et al. (2015a), when VEGF-A+VEGFR2 is formed, the levels of Delta are increased in the system.

Figure 5 shows that the opposite is also true, because the lower the concentration of free VEGF-A, the greater the agglomeration of VEGFR2, since the compound VEGF-A+VEGFR2 will not be formed and the receptor will not be activated, inhibiting angiogenesis. By relating these dynamics to the introduction of the drug Avastin® in the system, which is an angiogenesis inhibitor drug, it is known that Avastin® receives VEGF-A, with the concentration of this ligand being decreased, which makes the concentration of the free VEGFR2 receptor higher.

Mathematical analysis showed that the increase and decrease of VEGF-A does not significantly alter the concentration of VEGFR2 at the stalk equilibrium point. The concentrations of all proteins in the model remains practically constant.

Another analysis that can be taken from Figure 5 is that the decrease in VEGF-A causes the concentrations of VEGFR2 at the tip and I point the approach, indicating that physiological angiogenesis can be achieved when free VEGF in the extracellular matrix decreases, as expected.

Relationship between the influence of VEGF on angiogenesis: a quantitative study:

Alves et al. (2018) observed the growth of the vascular network in chicken embryos divided into two distinct groups: the control group and the treated group. The control group was used to extract quantitative parameters and that means that in this group the levels of VEGF-A were maintained to enable a physiological system. In the treated group, the drug Avastin® was applied to decrease VEGF signaling and this means that the values of free VEGF-A in the extracellular matrix were decreased causing the VEGFR2 receptor to increase.

To describe the differences between the network topologies, the following analyzes will present the behavior of the system in the control group and the group treated with Avastin®. The drug treated the group represents the group in which VEGF-A was restricted.

One of the analyzes carried out was the verification of the length between the bifurcations of blood vessels in the two groups of embryos. When verifying this metric, Alves et al. (2018) uses the means obtained for the control and treated groups. This result is shown below in Figure 6.

Figure 6 – The average length between bifurcations for the control and treated groups .

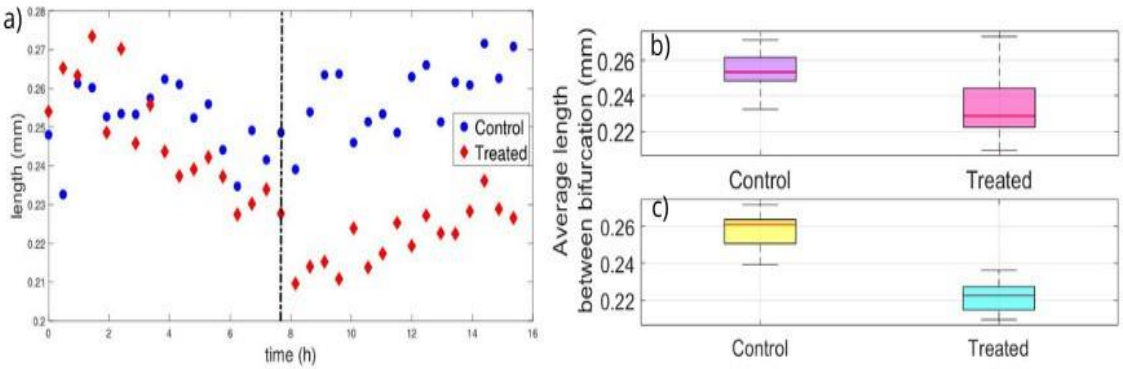

Source: Alves et al. (2018).

It can be seen from Figure 6a) that up to about 7.8 hours the average length between the bifurcations in the two groups grow similarly. At the initial stages the endothelial cells clusters interactions are very similar and don't have meaningful difference on the average length of the bifurcations. From 7.8 hours onwards, the mean length between blood vessel bifurcations in the treated group is shorter than in the control

group. This result is an indication that the action of Avastin® approaches the bifurcations in the treated group. In addition, Alves et al. (2018) identify that these differences between the control and treated groups are more expressive after 7.8 hours of the experiment.

To analyze the relative position between the groups and check whether the trend presented after 7.8 hours is statistically significant, the boxplot of the two groups was constructed together. For this, the interval from 0 to 15 hours of the experiment (Figure 6b) and the interval from 7.8 to 15 hours of the experiment were considered (Figure 6c).

According to Figure 6b), in the treated group the average length between bifurcations is shorter than in the control group. This difference becomes clearer when we analyze the data from 7.8 hours onwards. This suggests that Avastin® acts on the vascular network, bringing the nodules closer to the blood vessels. However, in the control group, VEGF-A microdomains serve as a guide for creating pathways that direct cell migration. As a result on the control group the microdomains of VEGF-A guide the connections and the vascular network displays a tree like topology. Probably, on the treated group, the Avastin bind to the microdomains of VEGF-A and broken pathways of cell migration. As a result, was obtained random connections and the vascular network displays a lattice like topology.

During the blood vessel growth process, VEGF-A binds to Avastin®, inhibiting VEGFR2. This indicates that this system in the treated group is moving towards the equilibrium point concentrations U represented in Figure 4, indicating instability. However, it is worth highlighting that the decrease in VEGF-A due to the action of the drug induces the unstable system to move towards physiological angiogenesis with characteristics of tip cells, as represented in Figure 5.

On the other hand, it is noted that the blood vessels in the control group have longer lengths between the bifurcations. This indicates that the lumen of the forming vessel is more elongated than in the treated group, because of the lateral induction process. Therefore, it can be said that the control group presents characteristics of stalk cells and tends to the stable equilibrium point of the stalk represented in Figure 4.

When cutting from 7.8 hours onwards, this behavior is clearer, as the boxplots remain without intersection and clearly, the average length between bifurcations is shorter in the treated group, confirming the trend shown in Figure 6a).

It is important to consider Figure 6c) because according to Alves et al. (2018) the largest connected cluster is formed after 5 hours of the experiment. Therefore, after 7.8

hours of the experiment, the angiogenesis process is considered and no longer the vasculogenesis process (which is the initial formation of blood vessels in embryos).

This highlights that it was possible to find a real solution for the equilibrium points of the mathematical model presented.

Another analysis carried out in Alves et al. (2018) refers to the average degree of the vertices as a function of time, that is, the number of connectivity of the nodes of the sample vessels, for the control and treated groups. The Figure 7 shows this representation.

Figure 7 – The average degree of the vertices for the control and treated groups .

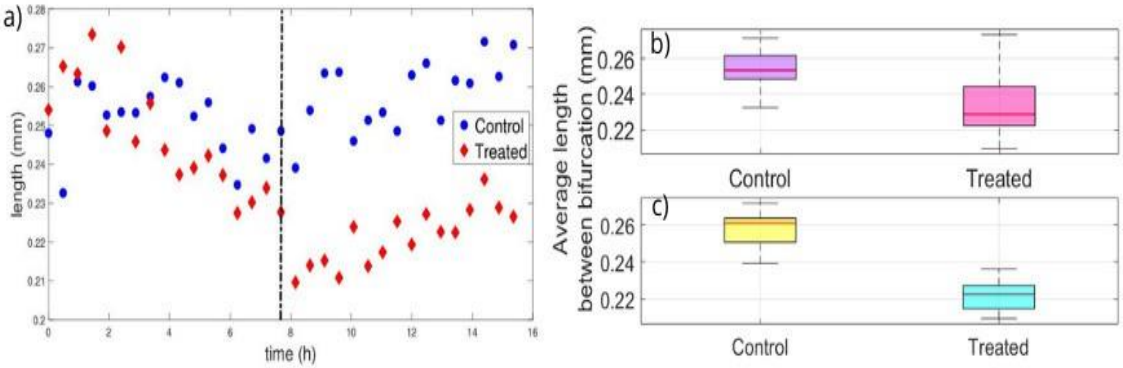

Source: Alves et al. (2018).

The dotted line in Figure 7 a) is a reference to track the 5 hour time, which according to Alves et al. (2018) is when the largest connected cluster is formed. The black arrows identify the time of 7.8 hours, which is the time close to saturation for both groups. After 7.8 hours of experiment large differences are identified between the network topologies of the two groups studied. The Figure 7 shows evidence of differences between the connectivity of the vascular network in the control and treated groups. This result corroborates the study presented in Jain (2005) which states that antiangiogenic drugs promote a reorganized vascular network to improve oxygenation and drug penetration into the system.

To analyze the relative position between the groups and check whether the trend presented in Figure 7a) after 7.8 hours is statistically significant, the two groups will be plotted in a boxplot together. For this, the interval from 0 to 15 hours of the experiment (Figure 7b) and the interval from 7.8 to 15 hours of the experiment (Figure 7c) will be considered.

The Figure 7b) presents the data referring to 15 hours of the experiment. There is an intersection between the boxes and a large scatter of data. However, the analysis after

7.8 hours of the experiment, in which data related to angiogenesis are effectively observed, shows independence between groups, symmetry and low dispersion in the data, as represented by Figure 7c).

It can be said that the treated group presents higher values for the average degree of the vertices. This shows that the trend shown in Figure 7a) from 7.8 hours onwards is statistically significant. According to Alves et al. (2018), Avastin® acts on the system making connections random, indicating the instability presented by the balance point that U represented in Figure 4. Furthermore, this greater connectivity capacity indicates that this unstable system is heading towards high concentrations of Delta and VEGFR2, which characterizes a tendency towards physiological angiogenesis given by the tip cells.

On the other hand, the lower connectivity in the control group shows that the concentrations of Delta and VEGFR2 in the system, which give rise to the tip cells that lead vessel growth, are lower than the concentrations of Notch, Jagged and NICD. Therefore, the control group system tends to the stalk equilibrium point that reflects a high incidence of stalk cells, as represented in Figure 4.

CONCLUSIONS

Understanding how new blood vessels grow according to signals emitted by signaling pathways is one of the essential factors in understanding angiogenesis and tumor development, and this field is an intense subject of research (Phng & Gerhardt, 2009).

When there is unrestrained growth of blood vessels designed to supply oxygen and nutrients to a tumor, it creates a favorable environment for tumor growth and metastasis (Siveen, 2017).

In this study, a mathematical model was proposed to describe the cellular dynamics involved in the angiogenesis process, based on the models presented in Boareto et al. (2015a) and Boareto et al. (2015b).

To validate the proposed model, the steps highlighted in Boareto et al. (2015b) were followed and the qualitative analyzes were similar, resulting in a simpler mathematical and functional model. The model presented here and based on the model by Boareto et al. (2015a) satisfactorily describes the concentrations of receptor proteins and ligands involved in cellular dynamics throughout the angiogenesis process.

In this study, the Notch and VEGF signaling pathways and the proteins that act in these pathways to promote angiogenesis were presented and analyzed.

Dysregulated Notch signaling can facilitate the emergence and proliferation of cancer stem cells, activating factors that promote cell survival and pathological angiogenesis Boareto et al. (2015b). This signaling pathway influences some types of cancer, such as breast and prostate cancer (Xiu & Liu, 2019; Wang, Li, Banerjee & Sarkar, 2009).

Likewise, VEGF signaling contributes to the self renewal and survival of cancer stem cells and is also related to several types of cancer, such as bone cancer (Chen et al., 2019; Mercurio, 2019).

Some studies such as Boareto et al. (2015a), Kumar et al. (2019) and Wang et al. (2009) indicate that high levels of Jagged proteins demonstrate characteristics associated with the emergence and main tenance of tumors. Overexpression of Jagged gives rise to a hybrid tip/stalk phenotype causing the fate of tip and stalk cells to be destabilized, making angiogenesis chaotic and generating excessive vessels inadequately perfused, which is one of the hallmarks of cancer. Furthermore, other studies, such as Chen et al. (2019), suggest that VEGF-A also has a great influence on the development of cancer cell metastases. Therefore, the importance of research that discusses the influence of ligand and receptor proteins during angiogenesis is considered.

The model proposed in this study disregards the performance of the fringe effect, as the initial analysis of the study showed that the inclusion of this effect was not decisive in the mathematical modeling proposed in Boareto et al. (2015a). However, for new and different approaches, it is suggested to evaluate the performance of the fringe according to the proposed objective.

The results presented in this work satisfactorily present the cellular dynamics of a single cell, which is immersed in an external environment in which other external concentrations are simulated, as done in Boareto et al. (2015a) and Boareto et al (2015b).

An important fact is that it was possible to correlate the system's equilibrium points with the Alves et al. (2018) experiments, in which the interaction of cell clusters in forming vascular networks was studied. In this sense, the abstract mathematical model was compared to the experimental study by Alves et al. (2018), in which it was possible to explain the formation of the vascular network. This relationship was obtained using the model and varying the amount of VEGF-A, given VEGF signaling. Once this was done, it was noticed that the balance of the system was disturbed and generated changes in the

blood vessel growth process. It was observed that the difference between the network topologies of the control group and the treated group became more evident after 7.8 hours of experiment.

The growth of new blood vessels in the control group observed by Alves et al. (2018) corresponds to a state of high concentration of stalk cells, which make up the formation of vessel walls. However, the growth of new blood vessels in the treated group, given the reflections of the model, reflects a tendency towards equilibrium point I, representing instability. Therefore, it was possible to obtain a solution for ordinary differential equations with fixed points that corresponds to the results obtained by Alves et al. (2018). Thus, it is highlighted that it was possible to find a real solution for the equilibrium points of the abstract model.

Just like healthy cells, malignant cells need oxygen and nutrients to survive and proliferate. These malignant cells reside close to blood vessels to more easily access the bloodstream (Lugano, Ramachandran & Dimberg, 2020). On this occasion, Notch, Delta, Jagged and VEGF-A have important roles in the development and cancer progression and analyzes to inhibit, target and manipulate Notch and VEGF signaling pathways are important for generating new types of cancer treatments (Xiu & Liu, 2009).

APPENDIX A. THE MATHEMATICAL MODEL

The mathematical model presented here is a model adapted from Boareto et al. (2015a). This model differs in that it does not add the performance of the fringe effect, which is an effect that model's part of the production of Notch to make it more apt to receive Delta instead of Jagged. Qualitative analyzes without fringe inclusion were analogous to Boareto et al. (2015a) making the model mathematically simpler and more functional.

Before talking about the model equations, it is important to talk about the shifted Hill equation, which is the equation that will represent the action of the NICD in increasing or restricting the rates of protein production in the cell nucleus. The shifted Hill equation is defined as:

$$H^s\left(X, \Lambda_{X,Y}\right) = H^-(X) + \Lambda_{X,Y} H^+(X) \quad \text{(A.1)}$$

where $H^-(X)$ is a constraint function, $H^+(X)$ is an activation function, and $\Lambda_{X,Y}$ denotes the change in the output of Y according to X. The restriction function and the activation function in the shifted Hill function are related to the parameters to be used in the model.

For the activation function (H^{S+}) we use $\lambda > 1$ and for the constraint function (H^{S-}) we have $\lambda = 0$. The shifted Hill function referring to NICD signaling is:

$$H^s(I,\lambda) = \frac{1}{1+\left(\frac{I}{I_0}\right)^n} + \lambda\frac{\left(\frac{I}{I_0}\right)^n}{1+\left(\frac{I}{I_0}\right)^n} \quad \text{(A.2)}$$

where n is the Hill exponent, which assumes different values for each protein depending on activation or restriction due to the action of the NICD. The parameter λ is also a constant that depends on whether the Hill-shifted function is positive (H^{S+} = activation function $\lambda > 0$) or negative (H^{S-} = constraint function $\lambda = 0$). The term I represents the concentration of NICD and I_0 is a constant.

When considering the inclusion of VEGF in the system, there is a contribution in the rate of production of proteins textit Delta. Delta is restricted by receptor signaling Notch, but is activated by VEGF signaling.

To include this activation of Delta, which also occurs by the action of the NICD, the shifted Hill function is analogous to Equation A.2. Therefore, the Hill function shifted in the function of VEGF is:

$$H^s(V,\lambda) = \frac{1}{1+\left(\frac{V}{V_0}\right)^n} + \lambda\frac{\left(\frac{V}{V_0}\right)^n}{1+\left(\frac{V}{V_0}\right)^n} \quad \text{(A.3)}$$

The term V represents the concentration of VEGF and V_0 is a constant.

When considering Equation A.2 for Notch and Jagged, the model assumes the positive shifted Hill function ($\lambda > 0$) and when considering Equation A.2 for Delta and VEGFR2 the shifted Hill function is negative ($\lambda = 0$). However, when considering the Equation A.3, the shifted Hill function becomes positive for Delta ($\lambda > 0$), since signaling via VEGF regulates the increase of this protein (Boareto et al., 2015a).

The shifted Hill functions, represented by Equation A.2 and Equation A.3, are efficient to describe state variations, being also useful to model the production of substances when their origins are being regulated by others (Fragoso, Ferreira & Marques, 2009).

Appendix A.1. Mathematical Model Details

Appendix A.1.1. Construction of the Notch equation

First, the equation for Notch will be built. For this, one must consider the link between Notch of a cell (N) and Delta of an external environment (D_{ext}) and this involves the interaction trans (k_t). This dynamic is represented by the Equation A.4.

$$[\mathrm{N}] + [D_{ext}] \longleftrightarrow [\mathrm{N}D_{ext}] \tag{A.4}$$

Note that Equation A.4 occurs in two directions. k_{t-} will be rendered right to left and k_{t+} left to right.

One must also consider the four factors that determine the variation of the protein Notch in a cell, which are:

- The NICD: which penetrates the cell nucleus activating the production of Notch. This makes the population of Notch concerning time to be proportional to the rate of production of Notch (N_0) multiplied by the shifted Hill function. This relationship is represented by Equation A.5, where $\lambda_{I,N}$ is the parameter represented by λ in Equation A.2 for the protein Notch and is related to the positive Hill function displaced by the NICD performance.

$$\frac{dN}{dt} \propto N_0 H^{s+}(I, \lambda_{I,N}) \tag{A.5}$$

- k_{t+}: if the Equation A.4 happens in the direction of k_{t+}, there is a decrease in population of N (and of D_{ext}) , which binds to D_{ext} to form another compound that also depends on D_{ext}. This relationship is represented by:

$$\frac{dN}{dt} \propto -k_{t+}\mathrm{N}D_{ext} \tag{A.6}$$

- k_{t-}: if the Equation A.4 happens in the direction of k_{t-}:, there is a population increase of N (and of D_{ext}):

$$\frac{dN}{dt} \propto +k_{t-}[\mathrm{N}D_{ext}] \tag{A.7}$$

- Natural degradation: the population of *Notch* decreases by a process of natural degradation that occurs at a rate γ:

$$\frac{dN}{dt} \propto -\gamma N \tag{A.8}$$

However, the inhibition *cis* can occur between *Notch* of the considered cell and *Delta* of the same cell. Like the interaction *trans*, the inhibition *cis* has different rates (k_{c+} and k_{c-}) and is represented by:

$$[N] + [D] \longleftrightarrow [ND] \quad \text{(A.9)}$$

According to Equation A.9, there are two more terms that will contribute $\frac{dN}{dt}$, which are:

- k_{c+}: is when the Equation A.9 happens from left to right. In this case, there will be a decrease in *Notch*, as *Notch* and *Delta* interact to form [*ND*]. This dynamic is represented by:

$$\frac{dN}{dt} \propto -k_{c+}ND \quad \text{(A.10)}$$

- k_{c-}: is when the Equation A.9 happens in a right-to-left direction. In this case, there will be an increase of *Notch* as [*ND*] breaks. This dynamic is represented by:

$$\frac{dN}{dt} \propto +k_{c-}[ND] \quad \text{(A.11)}$$

Putting together all the equations that represent $\frac{dN}{dt}$, so far, we have:

$$\frac{dN}{dt} = N_0 H^{s+}\left(I, \lambda_{I,N}\right) - N(k_{t+}D_{ext} + k_{c+}D) + k_{t-}[ND_{ext}] + k_{c-}[ND] - \gamma N \quad \text{(A.12)}$$

Equations representing the variations of $[ND_{ext}]$ and [*ND*] must also be considered.

For [ND_{ext}]:

- The production of this compound is increased at a rate k_{t+}, as represented by Equation A.4, and depends on the concentrations of [*N*] and $[D_{ext}]$:

$$\frac{d[ND_{ext}]}{dt} \propto +k_{t+}ND_{ext} \quad \text{(A.13)}$$

- However, the output of [ND_{ext}] is reduced by Equation A.4 when it happens from right to left:

$$\frac{d[ND_{ext}]}{dt} \propto -k_{t-}[ND_{ext}] \quad \text{(A.14)}$$

- There is also the degradation rate (k_l) of this compound in relation to a signal sent by the NICD:

$$\frac{d[ND_{ext}]}{dt} \propto -k_l[ND_{ext}] \quad \text{(A.15)}$$

Bringing together the Equation A.13, Equation A.14 and Equation A.15, we have:

$$\frac{d[ND_{ext}]}{dt} = +k_{t+}ND_{ext} - k_{t-}[ND_{ext}] - k_l[ND_{ext}] \quad \text{(A.16)}$$

To [ND]:

By arguments similar to those used to construct the equation of $[ND_{ext}]$, the variation of $[ND]$ is given by:

$$\frac{d[ND]}{dt} = +k_{c+}ND - k_{c-}[ND] - k_l[ND] \quad \text{(A.17)}$$

Assuming that these populations reach an equilibrium state (steady state), that is, $\frac{d[ND_{ext}]}{dt} = 0$ and $\frac{d[ND]}{dt} = 0$:

$$[ND_{ext}] = \frac{k_{t+}}{k_{t-} + k_l} ND_{ext} \quad \text{(A.18)}$$

$$[ND] = \frac{k_{c+}}{k_{c-}+k_l} ND \quad \text{(A.19)}$$

Replacing Equation A.18 and Equation A.19 into Equation A.12 and performing some mathematical manipulations, we have:

$$\frac{dN}{dt} = N_0 H^{s+}(I, \lambda_{I,N}) - k_{t+}ND_{ext}\left(\frac{k_l}{k_{t-} + k_l}\right) - k_{c+}ND\left(\frac{k_l}{k_{t-} + k_l}\right) - \gamma N \quad \text{(A.20)}$$

Defining $k_t = \frac{k_{t+}k_l}{k_{t-}+k_l}$ and $k_c = \frac{k_{c+}k_l}{k_{c-}+k_l}$ the equation from textit Notch will be:

$$\frac{dN}{dt} = N_0 H^{s+}(I, \lambda_{I,N}) - k_t ND_{ext} - k_{c+}ND - \gamma N \quad \text{(A.21)}$$

When *Notch* of the cell being analyzed (N) receives *Jagged* from the external environment (J_{ext}), the activation *trans* (k_t) and the NICD penetrates the nucleus of the cell that contains *Notch* activating the production of these two proteins. However, when the cell's *Notch* receives *Jagged* (J) from the same cell, the NICD is not triggered and both proteins are degraded by the *cis* (k_c) inhibition process. Analogous to the observations made when considering the dynamics between *Notch* and *Delta*, by adding *Jagged* in the Equation A.21, we have:

$$\frac{dN}{dt} = N_0 H^{s+}(I, \lambda_{I,N}) - k_t N(D_{ext} + J_{ext}) - k_{c+}N(D + J) - \gamma N \quad \text{(A.22)}$$

As the inclusion of VEGF does not directly affect the production of Notch, the mathematical model that represents *Notch* is given by Equation A.22.

Appendix A.1.2. Construction of the Delta equation

Now, the variation *Delta* of the cell in question will be modeled. The protein *Delta* (*D*) of this cell can interact with *Notch* from an external environment (N_{ext}), analogous to Equation A.4.

$$[N_{ext}] + [D] \leftrightarrow [N_{ext}D] \tag{A.23}$$

If the reaction of Equation A.23 occurs from left to right (k_{t+}), *Delta* decreases, but in the reverse direction (k_{t-}), *Delta* increases:

$$\frac{dD}{dt} \propto -k_{t+}N_{ext}D + k_{t-}[N_{ext}D] \tag{A.24}$$

The formation of NICD (*I*) restricts the production of *Delta*, so one must multiply the production rate of *Delta* (D_0) by the "negative" shifted Hill function:

$$H^{s-}\left(I, \lambda_{I,D}\right) = \frac{1}{1 + \left(\frac{I}{I_0}\right)^n} \tag{A.25}$$

Resulting in:

$$\frac{dD}{dt} \propto D_0 H^{s-}\left(I, \lambda_{I,D}\right) \tag{A.26}$$

One must also consider the natural degradation rate (γ) of *Delta*:

$$\frac{dD}{dt} \propto -\gamma D \tag{A.27}$$

In addition, the inhibition *cis* can occur between *Notch* and *Delta* of the same analyzed cell, like this:

$$\frac{dD}{dt} \propto -k_{c+}ND + k_{c-}[ND] \tag{A.28}$$

Putting together all the equations that represent $\frac{dD}{dt}$, so far, we have:

$$\frac{dD}{dt} = D_0 H^{s-}\left(I, \lambda_{I,D}\right) - k_{t+}N_{ext}D - k_{c+}ND + k_{t-}[N_{ext}D] + k_{c-}[ND] - \gamma D \tag{A.29}$$

The equations representing the variations of $[N_{ext}D]$ and [*ND*] must be considered, as was done for *Notch*.

When reviewing the arguments leading to Equation A.16, Equation A.17, Equation A.18 and Equation A.19, the Equation A.16 will be changed to:

$$\frac{d[N_{ext}\mathrm{D}]}{dt} = +k_{t+}N_{ext}D - k_{t-}[N_{ext}D] - k_l[N_{ext}D] \tag{A.30}$$

In the steady state, that is, $\frac{d[N_{ext}\mathrm{D}]}{dt} = 0$, there will be an equation analogous to Equation A.18, represented by:

$$[N_{ext}D] = \frac{k_{t+}}{k_{t-} + k_l} N_{ext}D \tag{A.31}$$

For [*ND*], Equation A.19 remains.

Replacing Equation A.31 and Equation A.19 into Equation A.29, the model is given by:

$$\frac{dD}{dt} = D_0 H^{s-}\left(I, \lambda_{I,D}\right) - k_t N_{ext} D - k_c N D - \gamma D \tag{A.32}$$

As already seen, it should be considered that the *Delta* production rate (D_0) is restricted by the NICD's performance by the *Notch* signaling pathway and increased by the NICD's effect by the VEGF signaling pathway. Therefore, to model the inclusion of VEGF performance in the concentration of *Delta*, just insert the term $H^{s+}\left(V, \lambda_{V,D}\right)$ by multiplying the production rate of *Delta* (D_0) in Equation A.32. Thus, the mathematical model for *Delta* will be:

$$\frac{dD}{dt} = D_0 H^{s-}\left(I, \lambda_{I,D}\right) H^{s+}\left(V, \lambda_{V,D}\right) - k_t N_{ext} D - k_c N D - \gamma D \tag{A.33}$$

Appendix A.1.3. Construction of the Jagged equation

Now, the *Jagged* variation of the cell being considered will be modeled. This analysis will be similar to the analysis performed for *Delta*.

The *Jagged* (J) protein of this cell can interact with *Notch* from an external environment (N_{ext}), so:

$$[N_{ext}] + [J] \longleftrightarrow [N_{ext}J] \tag{A.34}$$

If the reaction occurs from left to right (k_{t+}), *Jagged* int, but in reverse (k_{t-}), *Jagged* increases:

$$\frac{dJ}{dt} \propto k_{t+} N_{ext} J + k_{t-} [N_{ext}J] \tag{A.35}$$

Multiply a production taxon of *Jagged* (J_0) by the shifted Hill function:

$$\frac{dJ}{dt} \propto J_0 H^{s+}\left(I, \lambda_{I,J}\right) \tag{A.36}$$

Where $\lambda_{I,J}$ is the parameter represented by λ in Equation A.2 and is related to *Jagged*. One must also consider the natural degradation rate (γ) of *Jagged*.

$$\frac{dJ}{dt} \propto -\gamma J \tag{A.37}$$

In addition, *cis* inhibition may occur between *Notch* and *Jagged* of the same analyzed cell:

$$\frac{dJ}{dt} \propto -k_{c+} N J + k_{c-} [NJ] \tag{A.38}$$

By putting together all the equations that represent$\frac{dJ}{dt}$, so far, we have:

$$\frac{dJ}{dt} = J_0 H^{s+}\left(I, \Lambda_{I,J}\right) - k_{t+} N_{ext} J - k_{c+} NJ + k_{t-}[N_{ext}J] + k_{c-}[NJ] - \gamma J \quad \text{(A.39)}$$

Now, one must consider the equations that represent the variations of $[N_{ext}J]$ and $[NJ]$, as was done for *Notch* and *Delta*.

When reviewing the arguments leading to Equation A.16, Equation A.17, Equation A.18 and Equation A.19, the Equation A.30 will be given changed to:

$$\frac{d[N_{ext}J]}{dt} = +k_{t+} N_{ext} J - k_{t-}[N_{ext}J] - k_l[N_{ext}J] \quad \text{(A.40)}$$

In the steady state, that is, $\frac{d[N_{ext}J]}{dt} = 0$, there will be an equation analogous to Equation A.31, resulting in:

$$[N_{ext}J] = \frac{k_{t+}}{k_{t-} + k_l} N_{ext} J \quad \text{(A.41)}$$

For $[NJ]$, analogously to Equation A.41, we arrive at:

$$[NJ] = \frac{k_{c+}}{k_{c-} + k_l} NJ \quad \text{(A.42)}$$

By replacing Equation A.41 and Equation A.42 in Equation A.39, the mathematical model for *Jagged* will be given by:

$$\frac{dJ}{dt} = J_0 H^{s+}\left(I, \Lambda_{I,J}\right) - k_t N_{ext} J - k_c NJ - \gamma J \quad \text{(A.43)}$$

Appendix A.1.4. Construction of the NICD equation

For the NICD mathematical model, one must consider that a NICD output (I) affects *Notch*, *Delta* and *Jagged*. The NICD is only produced by the interaction textit trans between textit Notch of the analyzed cell and textit Delta and textit Jagged of the external environment (D_{ext} and J_{ext}):

$$\frac{dI}{dt} \propto +k_{t+} N D_{ext} - k_{t-}[ND_{ext}] + k_{t+} N J_{ext} - k_{t-}[NJ_{ext}] \quad \text{(A.44)}$$

There is also the NICD degradation rate which will be given by γ_I:

$$\frac{dI}{dt} \propto +k_{t+} N D_{ext} - k_{t-}[ND_{ext}] + k_{t+} N J_{ext} - k_{t-}[NJ_{ext}] - \gamma_I I \quad \text{(A.45)}$$

Since $[ND_{ext}]$ is given by Equation A.18, and by similar arguments $[NJ_{ext}]$ is found, in steady state, when performing some mathematical manipulations, the equation representing the NICD is:

$$\frac{dI}{dt} = k_t N(D_{ext} + J_{ext}) - \gamma_I I \tag{A.46}$$

Appendix A.1.5. Construction of the VEGF equation

Now, VEGF production will be considered. This factor, like the NICD, is only produced by the interaction *trans* (k_t) which in this case will occur when the cell's VEGFR2 receptor (VR) receives the VEGF-A ligand (V_{ext}):

$$\frac{dV}{dt} \propto +k_{t+} V_{ext} VR - k_{t-}[V_{ext} VR] \tag{A.47}$$

There is also the VEGF degradation rate that will be given by γ_I, so, incorporating this analysis, we have:

$$\frac{dV}{dt} \propto +k_{t+} V_{ext} VR - k_{t-}[V_{ext} VR] - \gamma_I V \tag{A.48}$$

By arguments similar to those used to determine $[ND_{ext}]$, we find the equation of the term $[V_{ext} VR]$ and performing some mathematical manipulations, the equation that represents the dynamics of VEGF will be given by:

$$\frac{dV}{dt} = k_t V_{ext} VR - \gamma_I V \tag{A.49}$$

Appendix A.1.6. Construction of the VEGFR2 equation

To model VEGFR2, it must be considered that its production rate (VR_0) is inhibited by the NICD, therefore:

$$\frac{dVR}{dt} \propto VR_0 H^{s-}(I, \lambda_{I,VR}) \tag{A.50}$$

There is also the natural degradation rate of VEGFR2 (γ):

$$\frac{dVR}{dt} \propto \gamma VR \tag{A.51}$$

Furthermore, this reaction only happens upon activation *trans* (k_t):

$$\frac{dVR}{dt} \propto -k_{t+} V_{ext} VR + k_{t-}[V_{ext} VR] \tag{A.52}$$

Combining the Equation A.50, Equation A.51 and Equation A.52, we have:

$$\frac{dVR}{dt} = VR_0 H^{s-}(I, \Lambda_{I,VR}) - k_{t+} V_{ext} VR + k_{t-}[V_{ext} VR] - \gamma VR \quad \text{(A.53)}$$

Considering the equation that represents the variation of $[V_{ext}VR]$, by arguments similar to those used for the *Notch* signaling, we arrive at Equation A.54, which represents the variation of the VEGFR2.

$$\frac{dVR}{dt} = VR_0 H^{s-}(I, \Lambda_{I,VR}) - k_t V_{ext} VR - \gamma VR \quad \text{(A.54)}$$

Appendix A.2. Parameters used

The parameters were taken from the studies of Boareto et al. (2015a). The Table 1 and Table 2 represents the values used.

Table 1 – Parameters used for the system composed of the equations for Notch, Delta, Jagged and NICD proteins.

Parameter	Value	Unit of Measurement
N_0	1600	Number of proteins / time (h)
J_0	1200	Number of proteins / time (h)
D_0	1800	Number of proteins / time (h)
I_0	200	Number of proteins / time (h)
N_{ext}	500	Number of proteins
J_{ext}	1750	Number of proteins
D_{ext}	0	Number of proteins
γ	0,1	$time^{-1}(h^{-1})$
γ_I	0,5	$time^{-1}(h^{-1})$
$\Lambda_{I,N} = \Lambda_{I,J}$	2	Dimensionless
$\Lambda_{I,D}$	0	Dimensionless
$n_N = n_D$	2	Dimensionless
n_J	5	Dimensionless
k_t	$5 * 10^{-5}$	$time^{-1}(h^{-1})$
k_c	$5 * 10^{-4}$	$time^{-1}(h^{-1})$

Source: Boareto et al. (2015b).

Table 2 – Parameters used for the system composed of the equations for Notch, Delta, Jagged, NICD, VEGF and VEGFR2 proteins.

Parameter	Value	Unit of Measurement
N_0	1200	Number of proteins / time (h)
J_0	800	Number of proteins / time (h)
$D_0 = VR_0$	1000	Number of proteins / time (h)
$I_0 = V_0$	200	Number of proteins / time (h)
$N_{ext} = J_{ext} = D_{ext} = V_{ext}$	2000	Number of proteins
γ	0,1	$time^{-1}(h^{-1})$
γ_I	0,5	$time^{-1}(h^{-1})$
$\Lambda_{I,N} = \Lambda_{I,J} = \Lambda_{V,D}$	2	Dimensionless
$\Lambda_{I,D} = \Lambda_{I,VR}$	0	Dimensionless
$n_N = n_D = n_{VR}$	2	Dimensionless
n_J	5	Dimensionless
k_t	$2{,}5 * 10^{-5}$	$time^{-1}(h^{-1})$
k_c	$5 * 10^{-4}$	$time^{-1}(h^{-1})$

Source: Boareto et al. (2015a).

REFERENCES

Alves, A., Mesquita, O., Gómez-Gardeñes, J., & Agero, U. (2018). Graph analysis of cell clusters forming vascular networks. *Royal Society Open Science*, *5*(3), 171592.

Andersson, E. R., Sandberg, R., & Lendahl, U. (2011). Notch signaling. *Development*, *138*(17), 3593–3612.

Apte, R. S., Chen, D. S., & Ferrara, N. (2019). VEGF in signaling and disease. *Cell*, *176*(6), 1248–1264.

Beatus, P., & Lendahl, U. (1998). Notch and neurogenesis. *Journal of Neuroscience Research*, *54*(2), 125–136.

Bhadada, S. V., Goyal, B. R., & Patel, M. M. (2011). Angiogenic targets for potential disorders. *Fundamental & Clinical Pharmacology*, *25*(1), 29–47.

Boareto, M., Jolly, M. K., Ben-Jacob, E., & Onuchic, J. N. (2015a). Jagged mediates differences in normal and tumor angiogenesis by affecting tip-stalk fate decision. *Proceedings of the National Academy of Sciences*, *112*(29), E3836–E3844.

Boareto, M., Jolly, M. K., Lu, M., Onuchic, J. N., Clementi, C., & Ben-Jacob, E. (2015b). Jagged–Delta asymmetry in Notch signaling can give rise to a sender/receiver hybrid phenotype. *Proceedings of the National Academy of Sciences*, 112(5), E402–E409.

Boareto, M., Jolly, M. K., Goldman, A., Pietilä, M., Mani, S., Sengupta, S., Ben-Jacob, E., Levine, H., & Onuchic, J. N. (2016). Notch-Jagged signalling can give rise to clusters of cells exhibiting a hybrid epithelial/mesenchymal phenotype. *Journal of the Royal Society Interface, 13*(118).

Bocci, F., Onuchic, J. N., & Jolly, M. K. (2020). Understanding the principles of pattern formation driven by Notch signaling by integrating experiments and theoretical models. *Frontiers in Physiology, 11*, 929.

Cheng, W. K., Oon, C. E., Kaur, G., Sainson, R. C., & Li, J.-L. (2022). Downregulation of manic fringe impedes angiogenesis and cell migration of renal carcinoma. *Microvascular Research, 142*, 104341.

Chen, S., Tang, C., Chie, M., Tsai, Y. F. C., Lu, Y., Chen, W., Lai, C., Wei, C., Tai, H., Chou, W., & Wang, S. (2019). Resistin facilitates VEGF-A dependent angiogenesis by inhibiting miR-16-5p in human chondrosarcoma cells. *Cell Death & Disease, 10*(31).

De Palma, M., Biziato, D., & Petrova, T. V. (2017). Microenvironmental regulation of tumour angiogenesis. *Nature Reviews Cancer, 17*(8), 457–474.

Domingues, J. S. (2010). *Modelo matemático e computacional do surgimento da angiogênese em tumores e sua conexão com as células-tronco* (Dissertação de mestrado, Centro Federal de Educação Tecnológica de Minas Gerais). Belo Horizonte, Brasil.

Flournoy, J., Ashkanani, S., & Chen, Y. (2022). Mechanical regulation of signal transduction in angiogenesis. *Frontiers in Cell and Developmental Biology, 10*, 1069783.

Folkman, J. (1984). *In biology of endothelial cells, Developments in Cardiovascular Medicine* (27).

Fouladzadeh, A., Dorraki, M., Min, K., Cockshell, M., Thompson, E., Verjans, J., & Abbott, D. (2021). The development of tumour vascular networks. *Communications Biology, 4*(1), 1111.

Fragoso, C. R., Ferreira, T. F., & Marques, D. M. (2009). *Modelagem Ecológica em Ecossistemas Aquáticos.* Oficina de Textos.

Freire, R. M. (2007). *Modelagem matemática para a simulação de estratégias de controle biológico da mosca-do-mediterrâneo* C. capitata (Diptera: Tephritidae) em plantações de citrus: Utilização de variáveis temporais e espaciais (Dissertação de mestrado, Universidade Estadual Paulista). Rio Claro, Brasil.

Funahashi, Y., Hernandez, S. L., Das, I., Ahn, A., Huang, J., Vorontchikhina, M., Sharma, A., Kanamaru, E., Borisenko, V., & DeSilva, D. M. (2008). A Notch1 ectodomain construct inhibits endothelial notch signaling, tumor growth, and angiogenesis. *Cancer Research, 68*(12), 4727–4735.

Geindreau, M., Bruchard, M., & Vegran, F. (2022). Role of cytokines and chemokines in angiogenesis in a tumor context. *Cancers, 14*(10), 2446.

Geudens, I., & Gerhardt, H. (2011). Coordinating cell behaviour during blood vessel formation. *Development, 138*(21), 4569–4583.

Huang, Y., & Nan, G. (2019). Oxidative stress induced angiogenesis. *Journal of Clinical Neuroscience, 63*, 13–16.

Jain, R. K. (2005). Normalization of tumor vasculature. *Science, 307*(5706), 58–62.

Jarriault, S., Brou, C., Logeat, F., Schroeter, E. H., Kopan, R., & Israel, A. (1995). Signalling downstream of activated mammalian Notch. *Nature, 377*, 355–358.

Kargozar, S., Baino, F., Hamzehlou, S., Hamblin, M. R., & Mozafari, M. (2020). Nanotechnology for angiogenesis: Opportunities and challenges. *Chemical Society Reviews, 49*(12), 5008–5057.

Kumar, S., Srivastav, R. K., Wilkes, D. W., Ross, T., Kim, S., Kowalski, J., Chatla, S., Zhang, Q., Nayak, A., Guha, M., Fuchs, S. Y., Thomas, C., & Chakrabarti, R. (2019). Estrogen dependent DLL1 mediated Notch signaling promotes luminal breast cancer. *Oncogene, 38*(1), 2092–2107.

Leite, N. M. G. (2009). *Modelagem matemática para a conexão entre células-tronco e câncer* (Dissertação de mestrado, Centro Federal de Educação Tecnológica de Minas Gerais). Belo Horizonte, Brasil.

Liao, B., & Oates, A. C. (2017). Delta-Notch signalling in segmentation. *Arthropod Structure & Development* 46 (3) 429–447.

Li, L., Krantz, I. D., Deng, Y., Genin, A., Banta, A. B., Collins, C. C., Qi, M., Trask, B. J., Kuo, W. L., & Cochran, J. (1997). Alagille syndrome is caused by mutations in human JAGGED1, which encodes a ligand for NOTCH1. *Nature Genetics*, 16(3), 243–251.

LoPilato, R. K., Kroeger, H., Mohan, S. K., Lauderdale, J. D., Grimsey, N., & Haltiwanger, R. S. (2023). Two Notch1 Ofucose sites have opposing functions in mouse retinal angiogenesis. *Glycobiology*, *33*(8), 661-672.

Lugano, R., Ramachandran, M., & Dimberg, A. (2020). Tumor angiogenesis. *Cellular and Molecular Life Sciences*, 77(9), 1745–1770.

Mercurio, A. M. (2019). VEGF/neuropilin signaling in cancer stem cells. *International Journal of Molecular Sciences*, 20(3), 1–12.

Moreira, E. A., & Ramos, R. (2021). Potencial antineoplásico dos fitocanabinóides. *Revista Multidisciplinar em Saúde*, 2(4), 137–137.

Mukherji, S. K. (2010). Bevacizumab (Avastin). *American Journal of Neuroradiology*, 31(2), 235–236.

Nascimento, D. L. (2021). *Modelo matemático para a angiogênese baseado na dinâmica das vias de sinalização Notch e VEGF* (Mestrado em Modelagem Matemática e Computacional). Centro Federal de Educação Tecnológica de Minas Gerais.

Nunes, D. N., Dias-Neto, E., Cardó-Vila, M., Edwards, J. K., Dobroff, A. S., Giordano, R. J., ... Pasqualini, R. (2015). Synchronous down-modulation of mir-17 family members is an early causative event in the retinal angiogenic switch. *Proceedings of the National Academy of Sciences*, 1–6.

Ozel, I., Duerig, I., Domnich, M., Lang, S., Pylaeva, E., & Jablonska, J. (2022). The good, the bad, and the ugly: Neutrophils, angiogenesis, and cancer. *Cancers*, 14(3), 536.

Patel, N. S., Li, J.-L., Generali, D., Poulsom, R., Cranston, D. W., & Harris, A. L. (2005). Up-regulation of Delta-like 4 ligand in human tumor vasculature and the role of basal expression in endothelial cell function. *Cancer Research*, 65(19), 8690–8697.

Phng, L., & Gerhardt, H. (2009). Angiogenesis. *Developmental Cell*, 16(2), 196–208.

Polacheck, W. J., Kutys, M. L., Yang, J., Eyckmans, J., Wu, Y., Vasavada, H., Hirschi, K. K., & Chen, C. S. (2017). A non-canonical Notch complex regulates adherens junctions and vascular barrier function. *Nature*, 552(7684), 258–262.

Qing, X., Xu, W., Liu, S., Chen, Z., Ye, C., & Zhang, Y. (2022). Molecular characteristics, clinical significance, and cancer immune interactions of angiogenesis associated genes in gastric cancer. *Frontiers in Immunology*, 13, 843077.

Qi, S., Deng, S., Lian, Z., & Yu, K. (2022). Novel drugs with high efficacy against tumor angiogenesis. *International Journal of Molecular Sciences*, 23(13), 6934.

Reiche, F. V., Bacal, F., & Mano, M. S. (2009). Inibidores da angiogênese e seus efeitos cardiovasculares no paciente com câncer: Importância do manejo multidisciplinar. *Revista da Sociedade de Cardiologia do Estado de São Paulo*, 19(4), 572–583.

Ross, D. A., & Kadesch, T. (2001). The Notch intracellular domain can function as a coactivator for LEF-1. *Molecular and Cellular Biology*, 21(22), 7537–7544.

Sarin, A., & Marcel, N. (2017). The Notch1-autophagy interaction: Regulating self-eating for survival. *Autophagy*, 13(2), 446–447.

Sayama, H. (2015). *Introduction to the modeling and analysis of complex systems*. Open SUNY Textbooks.

Scianna, M., Bell, C., & Preziosi, L. (2013). A review of mathematical models for the formation of vascular networks. *Journal of Theoretical Biology*, 333, 174–209.

Shibuya, M. (2011). Vascular endothelial growth factor (VEGF) and its receptor (VEGFR) signaling in angiogenesis: A crucial target for anti-and pro-angiogenic therapies. *Genes & Cancer*, 2(12), 1097–1105.

Siebel, C., & Lendahl, U. (2017). Notch signaling in development, tissue homeostasis, and disease. *Physiological Reviews*, 97, 1235–1294.

Silva, G. M. F. (2012). *Células-tronco e surgimento de tumores* (Dissertação de mestrado, Centro Federal de Educação Tecnológica de Minas Gerais). Belo Horizonte, Brasil.

Siveen, K. S., Prabhu, K., Krishnankutty, R., Kuttikrishnan, S., Tsakou, M., Alali, F. Q., Dermime, S., Mohammad, R. M., & Uddin, S. (2017). Vascular endothelial growth factor (VEGF) signaling in tumour vascularization. *Current Vascular Pharmacology*, 15(7), 339–351.

Troost, T., Binshtok, U., Sprinzak, D., & Klein, T. (2023). Cis-inhibition suppresses basal Notch signaling during sensory organ precursor selection. *Proceedings of the National Academy of Sciences*, 120(23), e2214535120.

Thurston, G., & Kitajewski, J. (2008). VEGF and delta-notch: Interacting signalling pathways in tumour angiogenesis. *British Journal of Cancer*, 99(8), 1204–1209.

Wang, Z., Li, Y., Banerjee, S., & Sarkar, F. H. (2009). Emerging role of Notch in stem cells and cancer. *Cancer Letters*, 279(1), 8–12.

Xiu, M. X., & Liu, Y. M. (2019). The role of oncogenic Notch2 signaling in cancer. *American Journal of Cancer Research*, 9(5), 837–854.

Zhou, B., Lin, W., Long, Y., Yang, Y., Zhang, H., Wu, K., & Chu, Q. (2022). Notch signaling pathway: Architecture, disease, and therapeutics. *Signal Transduction and Targeted Therapy*, 7(1), 95.